Available online at www.sciencedirect.com
ScienceDirect
Journal of Sound and Vibration 303 (2007) 185–194
JOURNAL OF SOUND AND VIBRATION
www.elsevier.com/locate/jsvi

Absorptive properties of three-dimensional phononic crystal

Honggang Zhao, Yaozong Liu*, Dianlong Yu, Gang Wang, Jihong Wen, Xisen Wen

Institute of Mechatronical Engineering, PBG Research Center, National University of Defense Technology, Changsha 410073, China

Received 23 May 2006; received in revised form 23 August 2006; accepted 7 January 2007
Available online 6 March 2007

Abstract

We consider the absorptive properties of three-dimensional phononic crystal (PC) composed of steel spheres arranged in viscoelastic rubber. The mode conversions during the Mie scattering of a single steel sphere in unbounded rubber are analyzed in detail. Then the multiple scattering (MS) and absorption effects induced by the simple cubic lattice and the viscosity of the rubber are investigated by the MS method. The results show that the shear and viscoelastic properties of the rubber are crucial, and the destructive interface induced by MS below each Bloch frequency enhances the absorption. Finally, the acoustic properties of finite PC slabs variation with the filling fraction and the incident angle are discussed for a variety of cases. The results show that the PC can be used as underwater anechoic material.

1. Introduction

Recently, there has been growing interest in a special type of inhomogeneous materials, known as phononic crystals (PCs). Within PCs the density and/or elastic coefficients vary periodically in space [1,2]. Based on the Bloch theory, several theoretical methods, such as the plane-wave expansion (PWE) method [1–4], the finite difference time domain (FDTD) method [5–7], finite element method [8,9] and the multiple scattering (MS) method [10–15], have been used to study the dispersion and the propagation of harmonic elastic waves through PC slabs. Numerous studies of PCs in one (1D), two (2D), and three dimensions (3D) have been reported in the last few years. Many results of physical interest, for example, the propagation modes, passbands, stopbands (or gaps), localization of classical waves, and effective homogeneous properties, etc., can be extracted from these studies. On the other hand, it relates to many applications such as the quantitative nondestructive evaluation, the design of sound absorptive materials, etc.

It is known that solid PCs possess several wave polarizations, i.e., one longitudinal and two transverse waves. The mode conversion among these waves and the sound absorption in viscous PC, however, has received considerably less attention. In fact, based on the theory for resonance scattering by isolated spherical inclusions, such as rubber sphere [16], metal sphere [17] or air sphere [18], ideas for the mechanism of the echo reduction have been discussed. More recently, Ivansson investigated the anechoic properties of viscoelastic

*Corresponding author. Tel./fax: +86 731 4574975.
E-mail address: yzliu@nudt.edu.cn (Y. Liu).

0022-460X/$ - see front matter © 2007 Published by Elsevier Ltd.
doi:10.1016/j.jsv.2007.01.004

rubber with periodically distributed spherical cavities as underwater coatings by rigorously accounting the MS effects [19,20]. Motivated by these studies, we try to show the fundamental absorbing mechanisms operating in PC, which is composed of a simple cubic lattice of nonoverlapping steel spheres arranged in viscoelastic rubber. The material combination chosen here is based on the principle that preferred in Ref. [17]. In the present investigation, we firstly investigate the efficiency of the mode conversion for an isolated steel sphere in unbounded rubber using an exact Mie scattering. Then the effects of the MS and the damping effects in PC are investigated by the MS method.

This paper is organized as follows. The model and the calculation method for solid-solid binary 3D PC are briefly outlined in Section 2. We discuss the numerical results in Section 3, and draw conclusions in Section 4.

2. Models and multiple scattering method

2.1. Models

Fig. 1 shows the model of the 3D PC considered in this paper under the Cartesian coordinates system. The layer spheres in XY plane are arranged infinitely in a two-dimensional square lattice defined by the primitive vectors $\mathbf{a}_1$ and $\mathbf{a}_2$ (see Fig. 1(a)). Fig. 1(c) shows the first Brillouin zone correspondingly. The finite PC slab can be viewed as a sequence of planes of spheres perpendicular to the Z-axis.

2.2. Mie scattering

The displacement for harmonic elastic wave propagation in homogeneous elastic medium represents the following time-independent equation

$$(\lambda + 2\mu)\nabla(\nabla \cdot \mathbf{u}) - \mu\nabla \times \nabla \times \mathbf{u} + \rho\omega^2\mathbf{u} = 0. \tag{1}$$

In spherical coordinates system, the solution can be decomposed into one longitudinal (**L** mode) and two transverse (**M** and **N** modes) solutions

$$\mathbf{u} = \mathbf{L} + \mathbf{M} + \mathbf{N}. \tag{2}$$

The spherical-wave solutions of the wave equation can be written in the generally form [10]

$$\mathbf{u}(\mathbf{r}) = \sum_{lm\sigma} [a_{lm\sigma}\mathbf{J}_{lm\sigma}(\mathbf{r}) + b_{lm\sigma}\mathbf{H}_{lm\sigma}(\mathbf{r})], \tag{3}$$

where $\sigma = 1, 2, 3$ correspond to $\mathbf{L}, \mathbf{M}, \mathbf{N}$ modes, respectively. $b_{lm\sigma}$ and $a_{lm\sigma}$ represent the expansion coefficients for the scattered and input waves, respectively. The relation between the coefficients $B = \{b_{lm\sigma}\}$ and $A = \{a_{lm\sigma}\}$ can be acquired by the solution of the Mie scattering with the following matrix form:

$$B = TA, \tag{4}$$

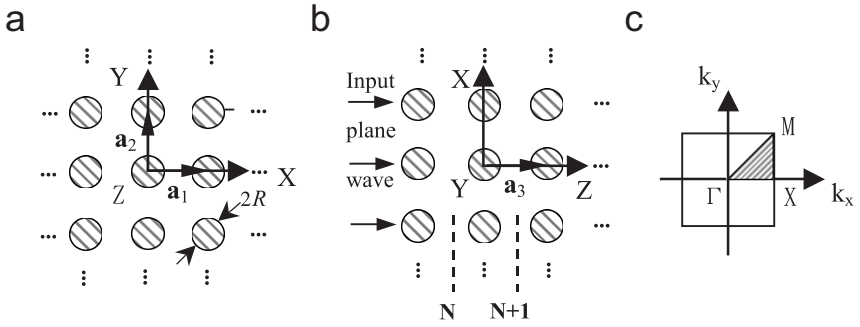

Fig. 1. The primitive vectors $\mathbf{a}_1$, $\mathbf{a}_2$, and $\mathbf{a}_3$ for the simple cubic lattice. (a,b) denote the lattice in XY-plane and out of XY-plane respectively, and (c) the first unreduced Brillouin zone of the array in XY-plane.

where $T = \{t_{lm\sigma l'm'\sigma'}\}$. The process to obtain the Mie scattering matrix (T) of a sphere is an eigenfunction expansion of the fields inside and outside the sphere. The fields are composed of infinite summations of spherical harmonics with unknown modal coefficients, which are then determined by the boundary conditions, i.e., the displacement and normal stress continuity at the interface. For spherical scatterer, the scattering matrix is independent of m and diagonal with l. The Mie scattering matrix for each partial waves of l order presents the following form:

$$\begin{bmatrix} LL & 0 & LN \\ 0 & MM & 0 \\ NL & 0 & NN \end{bmatrix}. \tag{5}$$

The meanings of the five nonzero elements are pellucid. For example, LL stands for the conversion from **L** to **L** mode during the scattering procedure, i.e., longitudinal incident wave scattered into a longitudinal outgoing wave. It shows that the **L** mode and the **N** mode are coupled to each other, while the **M** mode is decoupled.

2.3. Multiple scattering method

The MS method is a layer-by-layer approach for calculating the transmittance and reflectance for a finite slab with periodically arranged scatterers. For the central scatterer at the origin, the scattered wave

$$\mathbf{u}^{\mathrm{sc}}(\mathbf{r}) = \sum_{lm\sigma} b_{lm\sigma}\mathbf{H}_{lm\sigma}(\mathbf{r}) \tag{6}$$

is mainly determined by the overall incident wave, which includes two parts. One is the externally incident wave $\mathbf{u}^{in(e)}(\mathbf{r}) = \sum_{lm\sigma} a^{(e)}_{lm\sigma}\mathbf{J}_{lm\sigma}(\mathbf{r})$. The second part is the sum of all the scattered waves except that from the central scatterer. We obtain

$$\mathbf{u}^{in}(\mathbf{r}) - \mathbf{u}^{in(e)}(\mathbf{r}) = \sum_{\mathbf{r}_j \neq 0} \sum_{lm\sigma} b^j_{lm\sigma}\mathbf{H}^j_{lm\sigma}(\mathbf{r}_j), \tag{7}$$

where $\mathbf{r}_j$ refers to the position of the spatial point measured form scatterer j. According to the Bloch theorem, one obtains

$$b^j_{lm\sigma} = b_{lm\sigma}\,\exp(i\mathbf{k}_{\|}\cdot\mathbf{R}_j), \tag{8}$$

where $\mathbf{k}_{\|}$ is a reduced wave vector in the 2D Brillouin zone of the reciprocal lattice, and $\mathbf{R}_j$ represents the position of scatterer j. The coefficients of $\{b_{lm\sigma}\}$ are completely determined by $\{a^{(e)}_{lm\sigma}\}$ through the scattering matrix T. To get the transmittance and reflectance of the central layer between the artificial interfaces labeled with N and $N+1$ in Fig. 1(b), all the spherical-wave expansions of total scattering and input waves need to be transformed to plane waves as the general form:

$$\sum_{\mathbf{g}} \mathbf{U}^{\pm}_{\gamma g}\exp(i\mathbf{k}^{\pm}_{\gamma g}\mathbf{r}), \tag{9}$$

where $\mathbf{k}^{\pm}_{\gamma g} = (\mathbf{k}_{\|} + \mathbf{g}, \pm\sqrt{\gamma^2 - |\mathbf{k}_{\|} + \mathbf{g}|^2})$, $\gamma = \omega c_l^{-1}$for **L** mode and $\gamma = \omega c_t^{-1}$ for **N** and **M** modes, respectively, and the superscript $+(-)$ means that the incidence is along positive (negative) Z-axis. Then we can obtain the relations of the input and output waves for the central plane of scatterers as following:

$$\begin{aligned} \mathbf{U}^{+}(N+1) &= \mathbf{Q}^{\mathrm{I}}\mathbf{U}^{+}(N) + \mathbf{Q}^{\mathrm{II}}\mathbf{U}^{-}(N+1), \\ \mathbf{U}^{-}(N) &= \mathbf{Q}^{\mathrm{III}}\mathbf{U}^{+}(N) + \mathbf{Q}^{\mathrm{IV}}\mathbf{U}^{-}(N+1). \end{aligned} \tag{10}$$

For details one can refer to Refs. [11–14]. Once the matrices Q for one scattering layer are determined, one can easily obtain the Q matrices of a slab of N layers thick. As for the inter-layer periodicity along Z-axis, the Bloch-theory guarantees

$$\mathbf{U}^{\pm}(N+1) = \exp(i\mathbf{k}\cdot\mathbf{a}_3)\mathbf{U}^{\pm}(N), \tag{11}$$

where $\mathbf{a}_3$ is the primitive vector along positive z (see Fig. 1(b)), $\mathbf{k} = (\mathbf{k}_{||}, k_z(\omega, \mathbf{k}_{||}))$. After some algebra it yields a standard eigenfunction

$$\begin{pmatrix} \mathbf{Q}^{\mathrm{I}} & \mathbf{Q}^{\mathrm{II}} \\ -\left[\mathbf{Q}^{\mathrm{IV}}\right]^{-1}\mathbf{Q}^{\mathrm{III}}\mathbf{Q}^{\mathrm{I}} & \left[\mathbf{Q}^{\mathrm{IV}}\right]^{-1}\left[\mathbf{I} - \mathbf{Q}^{\mathrm{III}}\mathbf{Q}^{\mathrm{II}}\right] \end{pmatrix} \begin{pmatrix} \mathbf{U}^{+}(N) \\ \mathbf{U}^{-}(N+1) \end{pmatrix} = \exp(i\mathbf{k}\cdot\mathbf{a}_3) \begin{pmatrix} \mathbf{U}^{+}(N) \\ \mathbf{U}^{-}(N+1) \end{pmatrix}, \tag{12}$$

where $\mathbf{I}$ is a unit matrix. For given $\mathbf{k}_{||}$ and ω, we obtain the eigenvalues $k_z(\omega, \mathbf{k}_{||})$. The method outlined above accounts for the material viscosity via complex field equations, complex propagation vectors and the corresponding boundary conditions on the surface of the spheres. Under the condition of fully elasticity, the propagating wave (pass band) or evanescent wave (band gap) depends on real or complex of k_z. For a finite PC slab of thickness D, the attenuation of an incident wave is determined by the reflection mechanism induced by the evanescent wave. Roughly speaking, the amplitude of the wave decreases proportionally to exp(-Im[k_z]D) [14,15]. Im[k_z] (Re[k_z]) denotes the imaginary (real) part of k_z. Under the viscoelastic condition, Im[k_z] denotes the attenuation including the absorption effects [17].

3. Results and discussions

3.1. Mode conversion during the Mie scattering

Before dealing with the overall bulk wave behavior of PC, it will be useful to state briefly certain basic features of the acoustic scattering by a single isolated sphere. Fig. 2 shows the summations of the absolute values of T-matrix elements from $l = 1$ to 6 for a steel sphere ($\rho = 7890\,\mathrm{kg\,m^{-3}}$, $c_l = 5780\,\mathrm{m\,s^{-1}}$, and

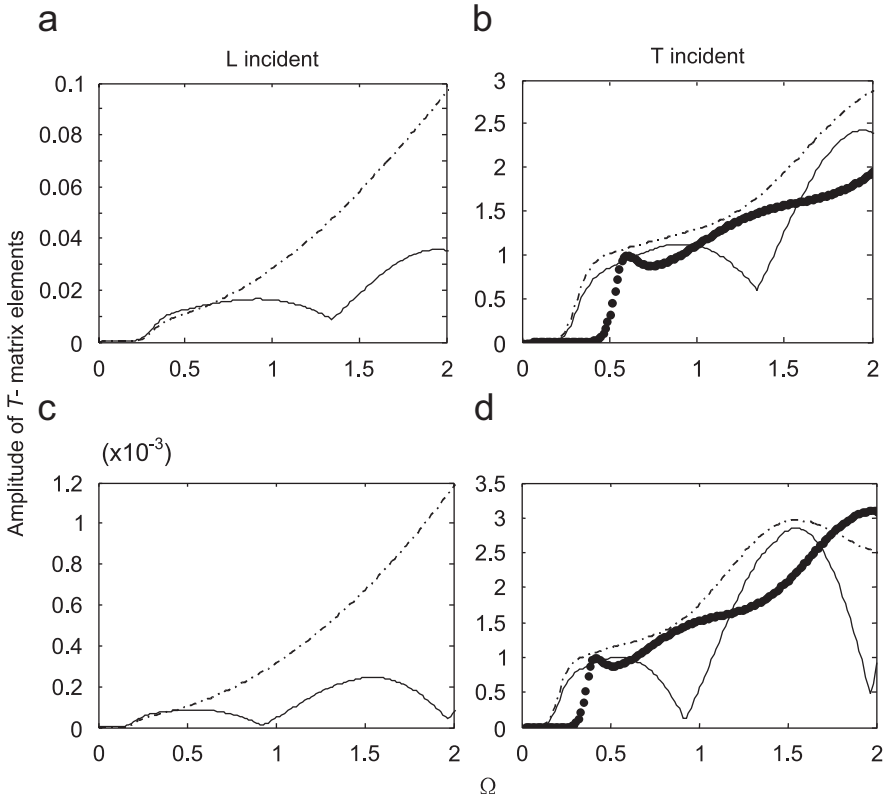

Fig. 2. The summations of the absolute values of T-matrix elements from $l = 1$ to 6 vs. frequency for an isolated steel sphere in unbounded rubber. (a,b) show the results for incident longitudinal and transverse waves respectively, and (c,d) are the same as (a,b) except that the transverse velocity of rubber is artificially decreased to $65\,\mathrm{m\,s^{-1}}$. In each, the dashed dot and solid lines are the cases without and with mode conversions between the **L** and **N** modes, respectively. The thick doted line denotes the MM element.

$c_t = 3220\,\mathrm{m\,s^{-1}}$) in unbounded rubber ($\rho = 1039\,\mathrm{kg\,m^{-3}}$, $c_l = 1470\,\mathrm{m\,s^{-1}}$, and $c_t = 360\,\mathrm{m\,s^{-1}}$). Here, the maximum of angular momentum cutoff $l_{\max} = 6$ yields accurate results in the given frequency range. In order to compare with what discussed in the following parts, the frequency Ω is scaled in units of fa/c_t. Here, a is the lattice constant of the simple cubic lattice adopted in the following part, and c_t denotes the transverse velocity of rubber. In the present computation, the ratio of the radius (R) of the sphere and the lattice constant is 0.36 and the viscosity of both components is neglected. For the low frequencies of interest, we find that the incident longitudinal wave does not convert a large fraction of energy into transverse wave. From Fig. 2(a) we can see that the incident energy flux is scattered by LN channel justly exceeds the LL channel near $\Omega = 0.45$. Under the transverse incidence, the amplitudes of T-matrix elements present more than one order of those for longitudinal incidence (see Fig. 2(b)). These observations suggest that the scattered energy tends to remain in transverse mode, which damp rapidly in rubber. Another consequence of the mode conversion is that the transverse waves tend to be scattered into directions away from the direction of the incident longitudinal wave and be channeled into propagation along the longer dimensions of PC slab, which enhances energy dissipation because loss increases exponentially with distance [16]. All these properties hint the reduction of the acoustic echo from a PC slab.

Generally, the transverse velocity of rubber is available within a large range, Figs. 2(c) and (d) show the cases of the Mie scattering when the transverse velocity of rubber is artificially decreased to $65\,\mathrm{m\,s^{-1}}$. It can be seen that these plots are relative stable in outlines as those in Figs. 2(a) and (b), respectively, but the mode-coupled frequency moves to lower frequency (and to much lower frequency in units of hertz). Unfortunately, a notable feature is the direct and mode conversion scatterings are greatly weakened under the longitudinal wave incidence, which will lead to less energy flux of transverse modes and less absorption.

3.2. The effects of multiple scattering

The Mie scattering from a single sphere may provide a primary picture of the absorption mechanism occurring within PC, but it does not fully address the effects due to the MS in PC. Here, we only consider the case of longitudinal incidence for the actual underwater case. Note here that the longitudinal wavelength is 4.1 times of that of the transverse wave in rubber at the same frequency. So the transverse wave interaction among the lattice will dominate the transmittance of the longitudinal waves at the low-frequency range considered here. The transverse wave, induced by mode conversion from longitudinal wave, is modulated by the periodicity in XY plane and satisfies the Bloch-theory. Below the first Bloch frequency (i.e., $\Omega = 1$, the definition of the Bloch frequency is given by Ref. [21]), the destructive interface among the lattice for the transverse wave interaction enhances the Mie scattering of the scatterer, which presents the "rigid body translational dipole resonance" [21]. The destructive interaction for the mode-converted transverse waves scattering blocks the wave transmission and induces the gap (see Figs. 3(a) and (b)). Another important consequence of the destructive interaction is the effective velocities of the PC, denoted by the slopes of the dispersion curves in Fig. 3(a), becomes slow near the dipole resonance. These observations suggest that the transverse mode of the scattered energy is greatly enhanced by the MS, which will yield good scattering absorption in viscoelastic PC.

3.3. The effects of viscosity

Generally, the viscosity would make the Lamé parameters (hence the velocities) be complex, i.e., $\lambda = \lambda_e - i\lambda_v$, $\mu = \mu_e - i\mu_v$. The real and imaginary parts, denoted by subscripts e and v, refer to the elastic and loss moduli, respectively. Here, we neglect the viscosity of steel since the loss for steel is much smaller than that of rubber. Two different viscous levels for rubber are adopted. They are $\lambda_v = 0.1\lambda_e$, $\mu_v = 0.1\mu_e$ for low viscosity and $\lambda_v = 0.1\lambda_e$, $\mu_v = 0.2\mu_e$ for high viscosity. For simplicity, it is provided that the viscoelastic properties of the components do not vary with frequency. Fig. 3(c) shows the attenuation, i.e., $\mathrm{Im}[k_z]$ vs. frequency for different viscous level. Compare with Fig. 3(b), it can be seen that the main effect of the viscosity shown as the attenuation is dependent on the frequency. In general, the attenuation increases as a function of frequency although there are some exceptions, which is especially obvious near the gap frequency domain.

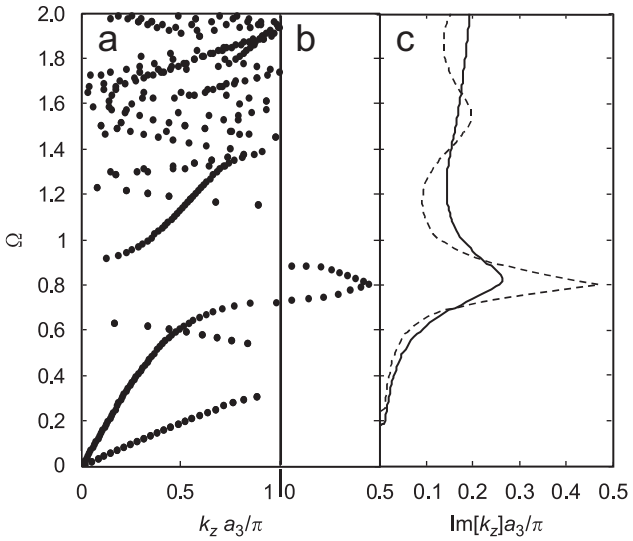

Fig. 3. Complex band structure of simple cubic lattice composed of steel spheres embedded in rubber. (a,b) represent the $\mathrm{Re}[k_z]a_3/\pi$ and $\mathrm{Im}[k_z]a_3/\pi$, respectively. The zeros of $\mathrm{Im}[k_z]$ are not plotted, (c) the attenuations with low and high viscosity in rubber are plotted with dashed and solid lines, respectively. In the present computation, R/a is 0.36, accordingly the filling fraction is 0.19.

When the value of imaginary parts of Lamé parameters increases, one may observe that the high viscous level almost washes everything out as if there were no inner scatterers in the system.

3.4. Acoustic properties of finite PC slab

By examination of the components of the T matrix one can see that there exists conversion from longitudinal to transverse wave modes. The MS slows the wave propagation and enhances the energy absorption. As a longitudinal wave propagates through the PC, more and more of the input energy would be converted to transverse modes, which damp rapidly in viscoelastic rubber. So the subsequent scattering does not convert a large fraction of the transverse wave energy back into the longitudinal wave. In this section, we shall show the actual acoustic properties of finite PC slabs. The slabs are immersed in infinite water, and a plane longitudinal wave incidence is exerted in one side. The two interfaces of water/rubber are both considered in present investigation. We show that the PC slab can successfully employ scattering and damping effects to reduce acoustic reflections as underwater coatings. The effects of the transverse velocity of rubber, filling fraction, and the incidence angle on the acoustic properties are also discussed.

Fig. 4 compares the acoustic properties of two PC slabs with different transverse velocities, i.e., (a) $65\,\mathrm{m\,s^{-1}}$ and (b) $360\,\mathrm{m\,s^{-1}}$, of rubber with low viscosity. The slabs used here and in the following parts are two-layer thick. We can see, as expected, that the lower absorbance (higher transmittance) exists in the slab where the rubber possessing the lower transverse velocity, which is mainly induced by the weak mode conversion during the Mie scattering (see Fig. 2(c)). The three dips in the transmittance near $\Omega = 0.73$, 1.20, and 1.70 are mainly induced by the resonance scattering because of the destructive scattering below the first three Bloch frequencies (i.e., $\Omega = 1$, $\sqrt{2}$, and $\sqrt{3}$), respectively. Near the resonant frequencies, the intense scattering of transverse wave attenuates the forward propagating wave, accompanied by the absorption peaks due to the viscosity. One can observe that three unobvious reflectance peaks correspond to those of the absorbance (see Fig. 4(a)). Here, the reflected wave includes two parts. One is the direct interface reflection. The other is the back scattering of direct conversion from the longitudinal incidence and back conversion from the damped transverse waves. Choosing moderate filling fraction and viscosity can reduce the reflectance (see the following parts). As for the rubber with transverse velocity $360\,\mathrm{m\,s^{-1}}$, the absorbance is high and the peaks are not obvious (see Fig. 4(b)), which is mainly induced by the higher efficiency of mode conversion into transverse wave during the Mie scattering (see Fig. 2).

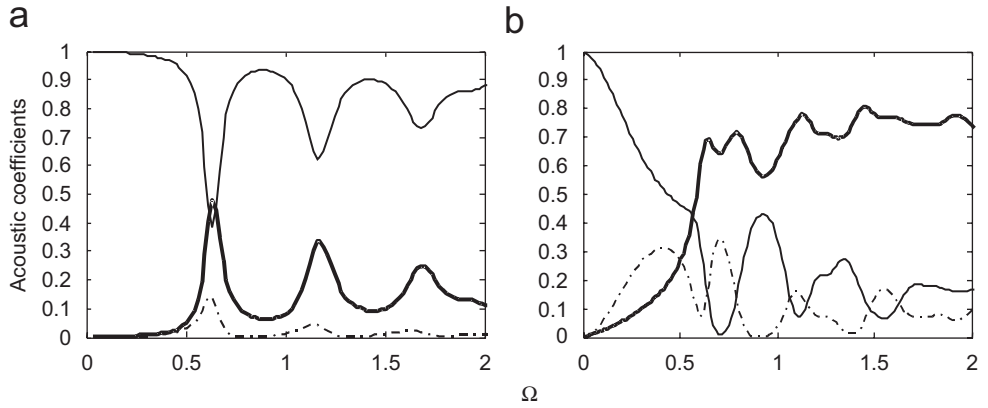

Fig. 4. Acoustic coefficients vs. frequency for a normally incident longitudinal wave through two-layer thick PC slabs with low viscosity. All the slabs possess the same lattice as Fig. 3. (a,b) represent the results for different transverse velocities of rubber with $65\,m\,s^{-1}$ and $360\,m\,s^{-1}$. In each, the thin solid, thick solid and dashed dot lines denote the transmittance, absorbance and reflectance, respectively.

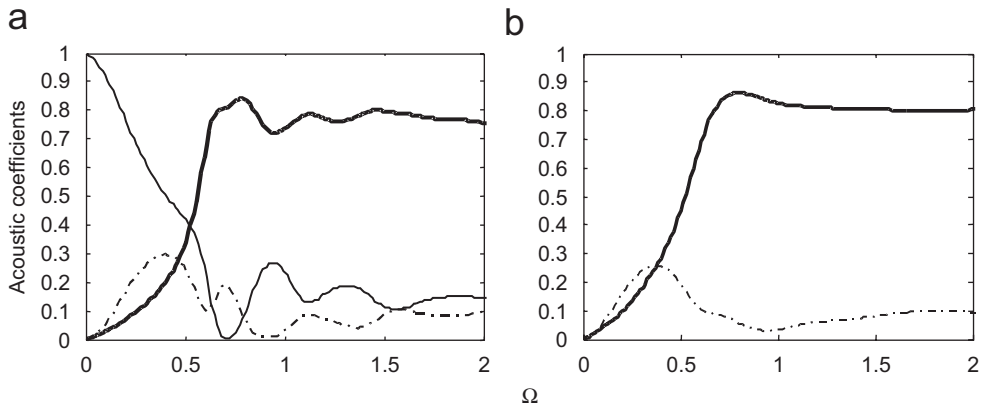

Fig. 5. The same as Fig. 4 (b) except that two viscous levels of rubber are adopted: (a) $\lambda_v = 0.1\lambda_e$, $\mu_v = 0.2\mu_e$, (b) $\lambda_v = 0.1\lambda_e$, $\mu_v = 0.5\mu_e$.

Based on Fig. 4(b), the effect of the viscosity of rubber on the acoustic properties of the slab is investigated. A higher viscosity level $\lambda_v = 0.1\lambda_e$, $\mu_v = 0.5\mu_e$ is adopted. Fig. 5 shows the acoustic properties of the slab with high viscosity in rubber. We can readily see that the absorbance is enhanced and the reflectance is depressed due to more energy being damped. And the oscillations in the absorbance, as other acoustic coefficients, gradually disappear. A notable feature is that the reflectance near $\Omega = 0.4$ is little depressed, which is mainly induced by the impedance mismatch induced by the relative high concentration of steel spheres ($R/a = 0.36$). The worse cases may occur at higher filling fraction, as shown in Fig. 6(d).

We have also looked at the variation of the acoustic coefficients with the filling fraction. From Fig. 6, one can see that the absorbance peak moves little to lower frequency with the sphere's radius increasing, which is mainly induced by the Mie scattering. From Fig. 7, we can readily see that the mode conversion by LN channel during the Mie scattering moves to lower frequency when increasing the radius of the sphere. But the absorbance is reduced by the impedance mismatch (due to the high impedance of spheres) and the volume reduction of the viscous rubber for energy loss (see Fig. 7). The preferable R/a ranges from 0.3 to 0.36 for the actual anechoic material.

What discussed above is based on the normal incidence, i.e., along Z-axis. Here, we investigate the effects of the incident angle on the acoustic properties. Fig. 8 shows the variation of the acoustic coefficients with the incidence angles. It is observed that the absorbance gets little larger with the incidence angle increasing. The

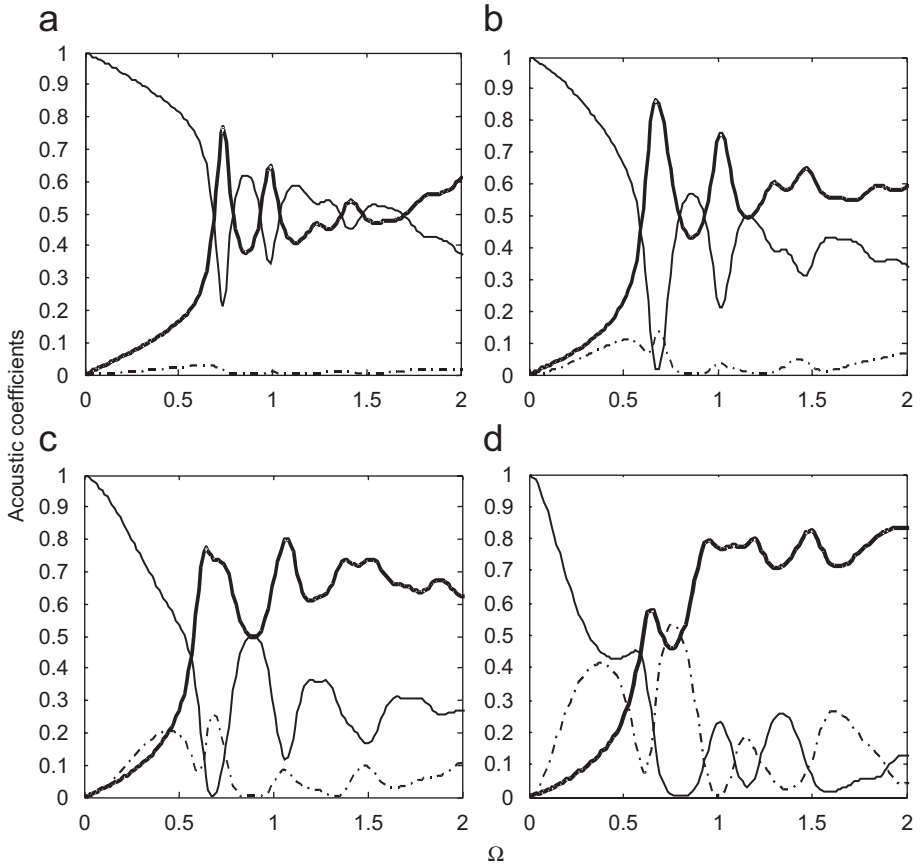

Fig. 6. The same as Fig. 4 (b) except that different radii of spheres are selected: $R/a =$ (a) 0.18, (b) 0.25, (c) 0.31, and (d) 0.40, respectively.

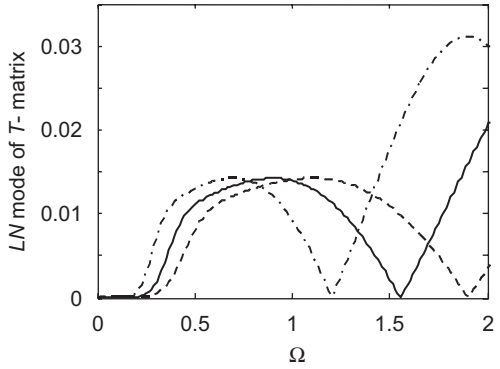

Fig. 7. Variation of summation of the absolute values of LN elements from $l = 1$ to 6 with the radius of the sphere. The ratios of the spherical radii and the lattice constant are 0.25 (dashed line), 0.31 (solid line) and 0.40 (dashed dot line), respectively.

reflectance at low frequency is reduced gradually. The reason may be that the incident component along XY plane, as a direct transverse wave incidence, increases with the incident angle.

4. Conclusions

We have shown the mode conversion of the isolated steel sphere in unbounded rubber. It shows that there exists coupling from longitudinal to transverse wave modes or vice versa. Then the effects of the MS and the

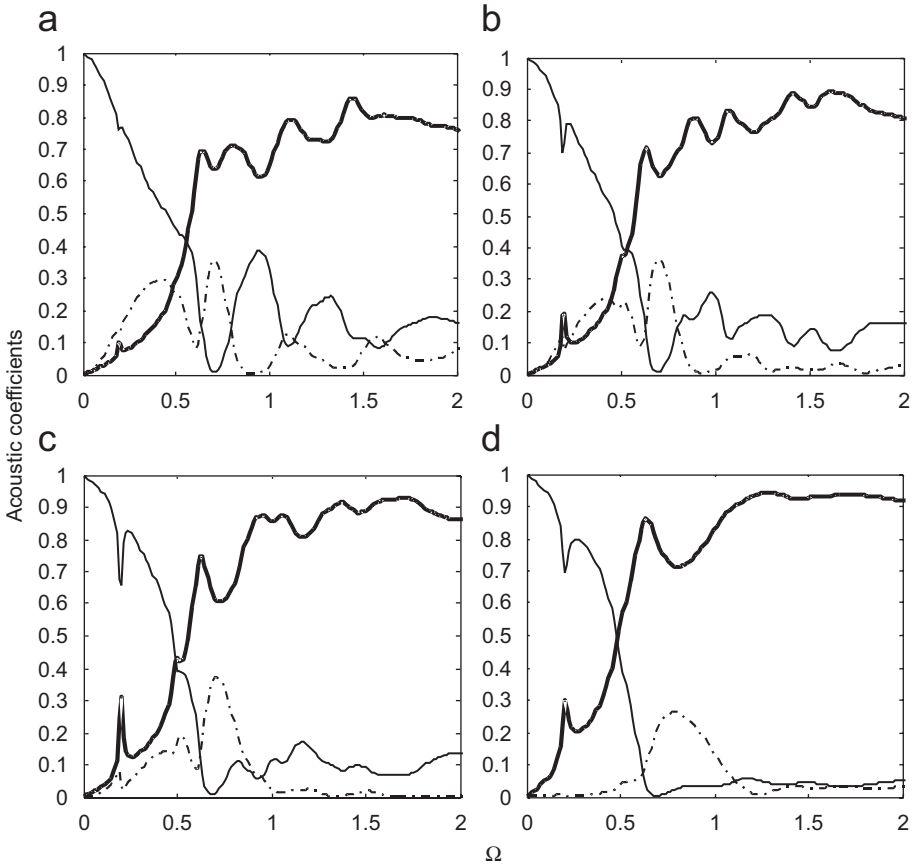

Fig. 8. The same as Fig. 4(b) except that the incident angles are (a) 15°, (b) 30°, (c) 45° and (d) 60°.

viscosity for PCs with simple cubic lattice of steel spheres arranged in viscoelastic rubber were investigated. As a longitudinal wave propagates through the PC, the destructive interface below each Bloch frequencies enhances the mode conversion to transverse wave, which damps rapidly in viscoelastic rubber and turns to heat. So the subsequent scattering does not convert a large fraction of the transverse wave energy back into the longitudinal wave. These results show the fundamental absorption mechanism induced by the MS and viscosity effects operating in PC. For the finite PC slab, it shows that the absorbance (reflectance) can be increased (decreased) by choosing moderate filling fraction and viscosity. For further optimal design, one may choose other lattice (such as face cubic lattice), material combinations and different layers combination (for example, the outer layer for impedance matching and the inner layer for absorption), etc.

Acknowledgments

This work was funded by the State Key Development Program for Basic Research (Grant No. 51307) of China.

References

[1] M.M. Sigalas, E.N. Economou, Elastic and acoustic wave band structure, *Journal of Sound and Vibration* 158 (1992) 377–382.
[2] M.S. Kushwaha, P. Halevi, L. Dobrzynski, B. Djafarirouhani, Acoustic band structure of periodic elastic composites, *Physical Review Letters* 71 (1993) 2022–2025.
[3] M.M. Sigalas, Elastic wave band gaps and defect states in two-dimensional composites, *Journal of the Acoustical Society of America* 101 (1997) 1256–1261.

[4] H.G. Zhao, Y.Z. Liu, G. Wang, J.H. Wen, D.L. Yu, X.Y. Han, X.S. Wen, Resonance modes and gap formation in a two-dimensional solid phononic crystal, *Physical Review B* 72 (2005) 12301.
[5] Y. Tanaka, Y. Tomoyasu, S. Tamura, Band structure of acoustic waves in phononic lattices: two-dimensional composites with large acoustic mismatch, *Physical Review B* 62 (2001) 7387–7392.
[6] M.M. Sigalas, N. Garcia, Theoretical study of three dimensional elastic band gaps with the finite-difference time-domain method, *Journal of Applied Physics* 87 (2000) 3122–3125.
[7] G. Wang, J.H. Wen, X.Y. Han, H.G. Zhao, Finite difference time domain method for the study of band gap in two-dimensional phononic crystals, *Acta Physica Sinica* 52 (2003) 1943.
[8] P. Langlet, Analysis of plane acoustic waves in passive periodic materials using the finite element method, *Journal of the Acoustical Society of America* 95 (1995) 2792–2799.
[9] W. Axmann, P. Kuchment, An efficient finite element method for computing spectra of photonic and acoustic band-gap materials I. Scalar case, *Journal of Computational Physics* 150 (1999) 468–481.
[10] Z. Liu, C.T. Chan, P. Sheng, Three-component elastic wave band-gap material, *Physical Review B* 65 (2002) 165116.
[11] I.E. Psarobas, N. Stefanou, A. Modinos, Scattering of elastic waves by periodic arrays of spherical bodies, *Physical Review B* 62 (2000) 278–291.
[12] Z. Liu, C.T. Chan, P. Sheng, A.L. Goertzen, J.H. Page, Elastic wave scattering by periodic structures of spherical objects: theory and experiment, *Physical Review B* 62 (2000).
[13] R. Sainidou, N. Stefanou, Green's function formalism for phononic crystals, *Physical Review B* 69 (2004) 64301.
[14] R. Sainidou, N. Stefanou, I.E. Psarobas, A. Modinos, A layer-multiple-scattering method for phononic crystals and heterostructures of such, *Computer Physics Communications* 166 (2005) 197–240.
[15] R. Sainidou, N. Stefanou, I.E. Psarobas, A. Modinos, The layer multiple-scattering method applied to phononic crystals, *Zeitschrift fuer Kristallographie* 220 (2005) 848–858.
[16] R. Lim, R.H. Hackman, A parametric analysis of attenuation mechanisms in composites designed for echo reduction, *Journal of the Acoustical Society of America* 87 (1990) 1076–1103.
[17] M.K. Hinders, B.A. Rhodes, T.M. Fang, Particle-loaded composites for acoustic anechoic coatings, *Journal of Sound and Vibration* 185 (1995) 219–246.
[18] G. Gaunaurd, K.P. Scharnhorst, H. Überall, Giant monopole resonances in the scattering of waves from gas-filled spherical cavities and bubbles, *Journal of the Acoustical Society of America* 65 (1979) 573–594.
[19] S. Ivansson, Numerical modeling for design of viscoelastic coatings with favorable sound absorbing properties, *Nonlinear Analysis* 63 (2005) e1541–e1550.
[20] S. Ivansson, Sound absorption by viscoelastic coatings with periodically distributed cavities, *Journal of the Acoustical Society of America* 119 (2006) 3558–3567.
[21] K. Maslov, V.K. Kinra, B.K. Henderson, Elastodynamic response of a coplanar periodic layer of elastic spherical inclusions, *Mechanics of Materials* 32 (2000) 785–795.